Biogeosciences Discuss., 8, 10797–10821, 2011
www.biogeosciences-discuss.net/8/10797/2011/
doi:10.5194/bgd-8-10797-2011

Biogeosciences Discussions

A model study on the sensitivity of surface ocean CO_2 pressure with respect to the CO_2 gas exchange rate

P. Landschützer[1,*], J. F. Tjiputra[1,2], K. Assmann[4], and C. Heinze[1,2,3]

[1]Geophysical Institute, University of Bergen, Bergen, Norway
[2]Bjerknes Centre for Climate Research, Bergen, Norway
[3]Uni Bjerknes Centre, Uni Research, Bergen, Norway
[4]British Antarctic Survey, High Cross, Madingley Road, Cambridge, UK
[*]now at: School of Environmental Sciences, University of East Anglia, Norwich, UK

Received: 3 October 2011 – Accepted: 20 October 2011 – Published: 8 November 2011

Correspondence to: P. Landschützer (p.landschutzer@uea.ac.uk)

Published by Copernicus Publications on behalf of the European Geosciences Union.

Abstract

Rising CO_2 concentrations in the atmosphere and a changing climate are expected to alter the air-sea CO_2 flux through changes in the respective control factors for gas exchange. In this study we determine the sensitivity of the CO_2 fluxes on the gas transfer velocity using the MICOM-HAMOCC isopycnic carbon cycle model. The monthly generated MICOM-HAMOCC output data are suitable to investigate seasonal variabilities concerning the exchange of CO_2. In a series of 3 sensitivity runs the wind dependent gas exchange rate is increased by 44 %, both in the northern and southern westerly regions, as well as in the equatorial area to investigate the effect of regional variations of the gas transfer rate on the air-sea fluxes and the distribution of the ocean surface pCO_2. For the period between 1948–2009, the results show that locally increasing gas transfer rates do not play an important role concerning the global uptake of carbon from the atmosphere. While effects on a global and annual scale are low, the regional and intra-annual variability shows remarkable variations in the gas fluxes and the surface pCO_2. An accurate quantification of the variable gas transfer velocity therefore provides a potential source to enhance model predictions over small spatial and temporal scales and to successfully reconcile model results on surface pCO_2 and air-sea CO_2 fluxes with observations.

1 Introduction

Gas exchange is one of the important links between the ocean and the atmosphere regarding biochemical cycles. It plays an important role for global climate in particular with respect to atmospheric greenhouse gases. The ocean is an important carbon reservoir and a major sink for anthropogenic CO_2 which has been emitted to the atmosphere (Solomon et al., 2007). The exchange process is controlled by the gas concentration difference between the atmosphere and the ocean surface layer, while the gas flux further depends on the specific gas transfer rate, which is the product of the gas

BGD
8, 10797–10821, 2011

transfer velocity and the gas solubility. In addition to the shifts in sea surface temperature and the surface wind stress, past and future greenhouse gas emissions provide changes in the ocean gas uptake. Trenberth et al. (2007) note that the strength of the mid-latitude winds have increased at least since the 1970s, especially in December, January and February. Model studies of Fyfe and Saenko (2006) confirm the strengthening and polewards shift of the Southern Hemisphere wind stress in the 20th century and predict the continuation of this trend during in the 21st century. These variations in the wind pattern provide changes in the gas uptake due to the wind dependency of the gas transfer velocity across the water-air interface. Studies of Zickfeld et al. (2007) and Tjiputra et al. (2010) predict an increasing carbon uptake in the high latitude Southern Hemisphere due to changes in the wind pattern and the resulting circulation changes. In contrast, a study by Le Quéré et al. (2007) based on both forward and inverse analysis methods estimate using synoptic atmospheric forcing that the Southern Ocean carbon uptake has weakened by 0.08 PgC per year per decade relative to the atmospheric increase of CO_2. This is attributed to the changing winds between 1981 and 2004 and is estimated to further weaken the Southern Ocean uptake strength in the near future. A study of Gruber et al. (2009) shows that there remain large uncertainties in the Southern Ocean carbon flux estimates. The study of Tjiputra et al. (2010) and numerous model studies presented in Meehl et al. (2007) predict a weakening of the Atlantic Meridional Overturning Circulation, which leads to a reduction of the CO_2 uptake in the North Atlantic, where according to Sabine et al. (2004) 23 % of the global anthropogenic carbon is stored. Observations suggest a decrease in the North Atlantic sink since 1990, linked to the phase changes in the North Atlantic Oscillation (Schuster and Watson, 2007; Watson et al., 2009).

Exploring the sensitivity of the carbon fluxes on the gas transfer rate can possibly improve our understanding of the uncertainties in future climate projections and the spread in results from different models on the ocean carbon cycle climate feedback (Friedlingstein et al., 2006). In the following study the effect of an increasing gas transfer rate is analyzed in 3 different ocean regions. The objective of the study is to assess

BGD
8, 10797–10821, 2011

the role of the gas transfer rate coefficient in influencing the global and regional uptake of CO_2 without changes in the ocean circulation.

2 The MICOM-HAMOCC isopycnic ocean carbon cycle model

We employ a state-of-the-art global biogeochemical ocean general circulation model (BOGCM) for our study. The physical component of the model is the Miami Isopycnic Coordinate Ocean Model based on the study by Bleck and Smith (1990) and Bleck et al. (1992). The current version of the model has been improved considerably as described in Bentsen et al. (2004) and Lohmann et al. (2009). The horizontal resolution of the model is approximately $2.4 \times 2.4^{\circ}$ with 34 isopycnic layers. In addition, the model includes a single non-isopycnic surface mixed layer, which provides the linkage between the atmospheric forcing and the ocean interior.

The ocean biogeochemistry model is the Hamburg Ocean Carbon Cycle (HAMOCC5) model. It is based on the original work of Maier-Reimer et al. (1993), which has been extensively improved and used in many studies (e.g., Six and Maier-Reimer, 1996; Aumont et al., 2003; Maier-Reimer et al., 2005). The current version of the model contains an NPZD-type ecosystem model with multi-nutrient limitation on the phytoplankton growth formulation (Maier-Reimer et al., 2005). The surface pCO_2 in the model is computed from the prognostic variables temperature, salinity, pressure, dissolved inorganic carbon (DIC), and alkalinity.

The model was originally spun up for 950 yr (Assmann et al., 2010). While 600 yr of the spin up were performed with a monthly NCEP-based climatology (Kalnay et al., 1996), another 350 yr spin up was performed with repeated passes of the NCEP Reanalysis 1950–1999 to obtain realistic sea-ice distributions, surface mixing and mixed layers. The model simulations were all restarted in 1948 from an initialization run starting in 1860 using NCEP atmospheric forcing of the year 1959, since no gridded physical atmospheric data exists prior to that date (Assmann et al., 2010).

BGD
8, 10797–10821, 2011

A more detailed model description as well as the evaluation of the model performance on a global scale is documented in Assmann et al. (2010). The model simulations performed in this study are forced by the monthly atmospheric fields from the NCEP reanalysis. For the air-sea CO_2 fluxes computation, observed atmospheric CO_2 concentration from the Mauna Loa observatory in Hawaii is prescribed in the model. Where available the monthly mean CO_2 and otherwise, the annual mean Mauna Loa CO_2 data are used to provide the atmospheric CO_2 concentration.

Gas Exchange

The gas flux between the ocean and the atmosphere is driven by the concentration difference between the atmosphere and the ocean and can be written, using the partial pressure difference of a gas as the thermodynamical driving force (Wanninkhof et al., 2009), as

$$F_{CO_2} = k_w \cdot S_{CO_2} \cdot (pCO_2^O - pCO_2^A) \quad (1)$$

where pCO_2^A expresses the CO_2 partial pressure in the atmosphere and pCO_2^O the partial pressure in the ocean surface. S_{CO_2} describes the solubility of CO_2 in seawater and can be derived according to Weiss (1974) from temperature and salinity via

$$\ln(S_{CO_2}) = A_1 + A_2 \cdot (100/T) + A_3 \cdot \ln(T/100) + s \cdot [B_1 + B_2 \cdot (T/100) + B_3 \cdot (T/100)^2] \quad (2)$$

where T denotes the temperature of the sea surface, s describes the salinity of the seawater and A_{1-3} and B_{1-3} are constants for the calculation in molar units. During the last decades several research projects focused on the formulation of the gas transfer velocity k_w. Deacon (1977) suggested in his formulation the transfer velocity k_w to be a function of the dimensionless Schmidt number (Sc), the numerical constant (β) factor and the friction velocity (u_*)

$$k_w = \beta^{-1} \cdot Sc^{-n} \cdot u_* \quad (3)$$

BGD
8, 10797–10821, 2011

Previous research focused on the quantitatively correct parameterizations of the gas transfer velocity (Liss and Merlivat, 1986; Wanninkhof, 1992; Wanninkhof and McGillis, 1999; Nightingale et al., 2000; Sweeney et al., 2007), resulting in different relationships between the gas transfer velocity and the wind speed. For the air-sea gas exchange, the model uses the formulation of Wanninkhof (1992) suggesting a quadratic relationship between the wind speed and k_w. Furthermore, in ice covered areas, the gas exchange is scaled down to the ice free parts of the grid cell (Maier-Reimer et al., 2005).

3 Sensitivity experiment: regional changes of the gas fluxes

The relations in Eqs. (2) and (3) suggest that the highest specific gas transfer rates ($k_s = k_w \cdot S_{CO_2}$) arise in low temperature and strong wind regions. To investigate the effect of an increasing gas exchange rate on the total uptake of CO_2, three different regions as listed in Table 1 were chosen. In the regions we substantially change the gas transfer velocity, however, do not take into account any change in the general pattern of gas exchange variability. Such a simplification is justified here as we first of all want to quantify the effect of a potential substantial change of the gas transfer on surface pCO_2 in general. The gas transfer rate in the various domains (Table 1) is increased in seperate experiments by 44 % which is equivalent to a 20 % increase in the wind speed as the model uses a quadratic relationship between the wind speed and the gas transfer velocity. The regions between 40–60° N and polewards of 40° S were selected because of their high specific gas transfer rates. The gas transfer was increased for the entire region polewards of 40° S including the ice covered area polewards of 60° S. The high specific gas transfer rates in these areas are caused by the influence of the strong westerly winds and the high gas solubilities due to the low sea surface temperatures. Besides the high specific gas transfer rates in these regions the air-sea disequilibrium suggests these regions to be mainly CO_2 uptake regions. In contrast, the third region between 20° S–20° N was selected because of the low specific gas transfer rate in the

BGD
8, 10797–10821, 2011

warmer equatorial waters and the air-sea disequilibrium identifying large parts to be outgassing areas.

All the sensitivity runs were examined with the same model settings as for the standard run. To avoid changes in the ocean surface circulation, the wind field was left unchanged. The model integration time starts in 1948 and ends in 2009. To present the results the year 2000 was chosen because of the available literature values from Takahashi et al. (2009) in that year to compare the total integrated carbon uptake.

4 Results

Annual mean CO_2 flux differences for the reference year 2000 between the sensitivity experiments and the model standard run are shown in Fig. 1. The strongest flux differences are in the northern and southern westerlies region where flux differences exceeding $\pm 2\,\mathrm{molC\,m^{-2}\,yr^{-1}}$ can be identified. In contrast the warm equatorial waters show flux differences less than $\pm 0.5\,\mathrm{molC\,m^{-2}\,yr^{-1}}$. Besides the differences in the experimental areas, changes in the carbon fluxes can likewise be discovered outside the experimental boarders. Water with higher carbon content gets transported by the surface currents resulting in an adaptation of the surface pCO_2 and the resulting gas fluxes outside the studied regions.

The increasing specific gas transfer rates influence the pCO_2 concentration as illustrated in Fig. 2. Changes in the surface pCO_2 result from modifications in the DIC concentration due to local variations of the carbon fluxes. Figure 2 indicates increasing partial pressures almost entirely in the uptake regions in the high latitudes and decreasing partial pressures in the equatorial region. The faster gas exchange results in pCO_2 differences up to ± 10 ppm with the exception of the ice covered area of the highest latitudes of the Southern Ocean. Assmann et al. (2010) point out that the sea-ice cover in the model is overestimated. Furthermore, the artificial high pCO_2 underneath the ice is caused by the upwelling of remineralized organic matter resulting from the export production which is computed too far south in the model.

BGD
8, 10797–10821, 2011

The effect of an enhanced gas transfer rate on the global integrated CO_2 flux is visualized in Fig. 3. The net carbon uptake in the global ocean undergoes very little changes in all 3 scenarios compared to the standard run, varying mainly between ±0.1 PgC. Compared to the different scenarios experiment G03 shows stronger year-to-year variation caused by the ice covered area below 60° S. A similar result can be identified observing the globally integrated mean pCO_2 difference between the runs, which vary less than ±2 ppm. Further analysis demonstrates that an increasing gas exchange rate does not simply show little effect on the global net uptake but has a notable effect on both the global upward and downward fluxes. Figure 4 illustrates the resulting fluxes plotted from 1990 onwards. Depending on the affected area the upward and downward fluxes increase simultaneously. The resulting fluxes for the year 2000 are displayed in Table 2. This result comes as a no surprise as the increase of the gas exchange rate shows its effect on both in- and outgassing. More surprising is that the slope shows no difference between the runs. By increasing the exchange rate of a net outgassing area one would expect a faster increase in the upward fluxes than in the downward fluxes. Instead, the lines only appear slightly shifted, leading to only small net differences between the runs.

To investigate the small annual differences an additional analysis for the year 2000 was performed on the intra-annual fluxes in the experimental regions. Figure 5 shows the monthly fluxes for the 3 experimental regions. The equatorial area shows a weak seasonal variation and describes a source for atmospheric CO_2 throughout the entire year, whereas both the high latitude regions are characterized by their intra-annual variability, but show a strong net uptake of CO_2 integrated over the entire year. The strong seasonality in the high latitudes of the Southern Hemisphere mainly results from the seasonal variation of the sea-ice.

Comparing the intra-annual fluxes of the standard run with the sensitivity runs, as illustrated in Fig. 5, indicates that the intra-annual signal gets strengthened in all cases. While the increasing gas transfer rate enhances the uptake from November until May in the Northern Hemisphere and from October until March in the Southern Ocean,

BGD
8, 10797–10821, 2011

the months of July until September and May until August indicate an equally strong increase of the outgassing fluxes of CO_2. The equatorial area shows generally less variation. This outcome suggests that the intra-annual difference is related to the pCO_2 variation shown in Fig. 2. The increasing gas transfer rate leads to a perturbation of the surface pCO_2 in relation to the standard run, leading to higher partial pressures of CO_2 in uptake areas and lower partial pressures in supersaturated areas. In the high latitudes it results in less uptake or increased outgassing in months of low air-sea disequilibrium, whereas the effect of the increased gas transfer rate dominates in months where the air sea disequilibrium is high.

Integrating the monthly fluxes between 40–60° N for both the model standard and the sensitivity run G02 results in a net flux difference of −67 TgC for the year 2000, where −46 TgC is the contribution of the Atlantic and −21 TgC of the Pacific. This is more than twice as much as the −23 TgC calculated from Table 2 for the global ocean. The minus signs indicate more uptake by the ocean. These differences arise from the surface transport of water with high CO_2 concentration outside the experimental domain of artificially adjusted gas transfer velocities, where the gas exchange slows down due to a lower CO_2 disequilibrium (prescribed atmospheric pCO_2 minus increasing ocean pCO_2 outside the experimental domain) and unchanged gas transfer rate. A different result can be identified in the Southern Ocean. The integrated carbon flux difference for the experimental region G03 between the standard run (−1406 TgC) and the sensitivity run (−1344 TgC) is 62 TgC, hence, the increasing gas transfer rate leads to decreasing uptake in the year 2000. Figure 3 shows that this differs from year to year. Again, the identified flux deviates from the global net difference in Table 2, suggesting that transport of high CO_2 water equatorwards causes the global difference. Likewise, the equatorial region from experiment G04 shows a net decrease in the outgassing flux of −4 TgC in the year 2000 due to the increasing CO_2 partial pressure.

To investigate whether changing the gas transfer rate can improve regional model prediction, we compared the results from the model runs with the climatology of Takahashi et al. (2009) for the year 2000. The model output data were binned to the same

BGD
8, 10797–10821, 2011

$4 \times 5^{\circ}$ grid boxes as presented for the climatology. Figure 6 shows the zonal averaged pCO_2 and CO_2 flux differences between the model runs compared to the Takahashi et al. (2009) data. The results from the sensitivity runs relative to the model standard run are plotted only in those latitudes where they differ from the standard run.

While there is large disagreement between the model fluxes and the climatological data in the Southern Hemisphere, differences in the Northern Hemisphere mainly do not exceed $\pm 50\,\mathrm{TgC\,yr^{-1}}$. Besides the good correlation between the fluxes northwards of 30° S ($R = 0.88$), the latitudes in the Southern Hemisphere southwards of 30° S show a poor correlation ($R = 0.23$) which slightly improves by the increasing gas exchange rate in experiment G03 ($R = 0.27$). Figure 6 shows that both pCO_2 and CO_2 flux minima are shifted south relative to the observations and below 60° S the ice cover causes the strongest disagreements. Therefore, in the following analysis, G03 is analyzed only between 40–60° S. In addition to the small local improvements between the equator and 20° S in experiment G04, Fig. 6 illustrates a remarkable deterioration resulting from experiment G02 at 40° N due to the enhanced carbon fluxes. Beside the strong pCO_2 difference in the ice covered area of the Southern Ocean the strongest disagreement between the model outputs and the climatology data lie in the mid latitudes in both hemispheres and the high latitudes in the Northern Hemisphere.

Stow et al. (2009) present a series of statistical tools to test the quality of the model output compared to observations. Some of these tools are used here to further investigate if the sensitivity runs improve the model prediction compared to the Takahashi et al. (2009) data for every zonal band. The results for the experimental areas are listed in Table 3. While the correlation coefficients between the CO_2 fluxes indicate that both the model and the sensitivity runs presents the climatology well between 40–60° N and between 20° S–20° N, the correlation is negative between 40–60° S due to the southward shift in the export production (Assmann et al., 2010). The root mean squared error (RMSE) and the average absolute error (AAE) results show that experiment G03 and G04 both decrease the discrepancies between model and observations, whereas experiment G02 shows and increasing bias. The model efficiency (MEF) indicates

BGD
8, 10797–10821, 2011

the accuracy of the model prediction relative to the average of the observations (Stow et al., 2009). A value close to 1 indicates a close match between model data and observations, whereas a value close to 0 states that the model predicts the observations not better than the mean of the observations. Negative values indicate that the observational mean would be a better predictor than the model output. Table 3 shows that model predictions are best between 20° S–20° N and get improved by the sensitivity experiment. A slight improvement can be discovered from experiment G03, whereas the results show that the observation mean is a much better predictor between 40–60° S due to the shift in the biology. The area 40–60° N is slightly better represented by the mean of the observations, whereas sensitivity run G02 shows a strong degradation of the model performance. The last result illustrates the potential to improve, or in this example rather deteriorate, the model prediction by adjusting the gas transfer rate in certain regions.

The pCO_2 RMSE and the AAE again show the largest model data discrepancies 40–60° S, whilst the errors are in general smaller between 40–60° N than between 20° S–20° N. The MEF indicates the same trend as before for the CO_2 flux. Experiment G03 and G04 represent the observation patterns better than the standard run, whereas G02 leads to a degradation of the model performance. Figure 6 reveals that both climatological CO_2 fluxes and pCO_2 data are lower between 40–60° N compared to the standard run, whilst the increasing gas exchange rate in G02 leads to increasing fluxes and partial pressures relative to the model standard run. A decreasing gas transfer rate in contrast would potentionally lead to a better model performance in experiment region G02. Additionally, due to the stronger inter-annual variation of the CO_2 fluxes in G03 the model mean results from the years 1995 to 2004 were compared to the Takahashi climatology (not shown). The results indicate that averaged over the 10 yr period the G03 outputs show higher uptake fluxes compared to the model standard run and therefore do not improve the model performance for the CO_2 fluxes, whereas the pCO_2 values only slightly differ from the numbers obtained in Table 3.

BGD
8, 10797–10821, 2011

5 Conclusions

The model results indicate that regional changes in the gas transfer rate, as they are applied in this study, do not strongly effect the global air-sea net flux of CO_2 on the long run. The enhanced regional gas fluxes lead to a perturbation in the surface pCO_2 relative to the model standard run, resulting in a negative flux feedback as the concentration difference between the atmosphere and the ocean is the driving factor for the gas exchange. We therefore conclude that changes in the ocean carbon uptake are dominated by the changes in the ocean circulation rather than the gas transfer coefficient.

A comparison with climatology data from Takahashi et al. (2009) shows that an increasing gas transfer rate of 44 % in the experimental areas does not substantionally improve the model predictions in the higher latitudes of the Southern Hemisphere where the model data and the climatology data are poorly correlated. The results in the equatorial area and the Northern Hemisphere instead do support the idea that local enhancements of the gas transfer rate have the potential to improve local model predictions by adjusting the gas transfer rate.

Furthermore, the study on the intra-annual variation between the sensitivity runs suggests that enhancements, some of them which are not considered in this study, could improve the local model performance relative to climatology data. Wanninkhof et al. (2009) suggest the gas exchange to be affected by naturally occurring surfactants, rain and bubble effects. An estimation of Woolf (1997) suggests a bubble contribution of 30 % on the global gas transfer velocity. Local model prediction results would undoubtedly benefit from including these effects.

This means, that after all, more detailed descriptions of variations in gas transfer velocities may have to be taken into account in advanced data assimilation schemes for parameter optimisations in biogeochemical ocean models. An omission of these descriptions may still result in acceptable global CO_2 uptake rates, but other processes than gas exchange may be corretced erroneously in order to correct locally for insufficient model representations of air-sea gas exchange processes.

BGD
8, 10797–10821, 2011

Acknowledgements. Supercomputer CPU time through NOTUR (Norwegian Metacenter for Computational Science) project nn2980k and file storage through NorStore (Norwegian Storage Infrastructure) project ns2980k, which made this study possible, are gratefully acknowledged. The research leading to these results has received funding from the European Community's Seventh Framework Programme (FP7/2007-2013) under grant agreement no. 238366. This study was co-sponsored by the EU FP7 project COMBINE (grant agreement no. 226520) and the EU FP7 coordination action COCOS (grant agreement no. 212196).

References

Assmann, K. M., Bentsen, M., Segschneider, J., and Heinze, C.: An isopycnic ocean carbon cycle model, Geosci. Model Dev., 3, 143–167, doi:10.5194/gmd-3-143-2010, 2010. 10800, 10801, 10803, 10806

Aumont, O., Maier-Reimer, E., Blain, S., and Monfray, P.: An ecosystem model of the global ocean including Fe, Si, P colimitations, Global Biochem. Cy., 17, 23, doi:10.1029/2001GB001745, 2003. 10800

Bentsen, M., Drange, H., Furevik, T., and Zhou, T.: Simulated variability of the Atlantic meridional overturning circulation, Clim. Dynam., 22, 701–721, 2004. 10800

Bleck, R. and Smith, L. T.: A wind driven Isopycnic Coordinate Model of the North and Equatorial Atlantic Ocean. 1 Model Development and Supporting Experiments, J. Geophys. Res., 95, 3273–3285, 1990. 10800

Bleck, R., Rooth, C., Hu, D., and Smith, L. T.: Salinity-driven Thermocline Transients in a Wind- and Thermohaline-forced Isopycnic oordinate Model in the North Atlantic, J. Phys. Oceanogr., 22, 1486–1505, 1992. 10800

Deacon, E. L.: Gas transfer to and across an air-water interface, Tellus, 29, 363–374, doi:10.1111/j.2153-3490.1977.tb00746.x, 1977. 10801

Friedlingstein, P., Cox, P., Betts, R., Bopp, L., von Bloh, W., Brovkin, V., Cadule, P., Doney, S., Eby, M., Fung, I., Bala, G., John, J., Jones, C., Joos, F., Kato, T., Kawamiya, M., Knorr, W., Lindsay, K., Matthews, H. D., Raddatz, T., Rayner, P., Reick, C., Roeckner, E., Schnitzler, K.-G., Schnur, R., Strassmann, K., Weaver, A. J., Yoshikawa, C., and Zeng, N.: ClimateCarbon Cycle Feedback Analysis: Results from the C4MIP Model Intercomparison, J. Climate, 19, 3337–3353, doi:10.1175/JCLI3800.1, 2006. 10799

BGD

8, 10797–10821, 2011

Fyfe, J. C. and Saenko, O. A.: Simulated changes in the extratropical Southern Hemisphere winds and currents, Geophys. Res. Lett., 33, L06701, doi:10.1029/2005GL025332, 2006. 10799

Gruber, N., Gloor, M., Mikaloff Fletcher, S. E., Doney, S. C., Dutkiewicz, S., Follows, M. J., Gerber, M., Jacobson, A. R., Joos, F., Lindsay, K., Menemenlis, D., Mouchet, A., Müller, S. A., Sarmiento, J. L., and Takahashi, T.: Oceanic sources, sinks, and transport of atmospheric CO_2, Global Biochem. Cy., 23, GB1005, doi:10.1029/2008GB003349, 2009. 10799

Kalnay, E., Kanamitsu, M., Kistler, R., Collins, W., Deaven, D., Gandin, L., Iredell, M., Saha, S., White, G., Woollen, J., Zhu, Y., Chelliah, M., Ebisuzaki, W., Higgins, W., Janowiak, J., Mo, K. C., Ropelewski, C., Wang, J., Leetmaa, A., Reynolds, R., Jenne, R., and Joseph, D.: The NCEP/NCAR 40-year reanalysis project, B. Am. Meteorol. Soc., 77, 437–471, doi:10.1175/1520-0477(1996)077<0437:TNYRP>2.0.CO;2, 1996. 10800

Le Quéré, C., Rödenbeck, C., Buitenhuis, E. T., Conway, T. J., Langenfelds, R., Gomez, A., Labuschagne, C., Ramonet, M., Nakazawa, T., Metzl, N., Gillett, N., and Heimann, M.: Saturation of the Southern Ocean CO_2 Sink Due to Recent Climate Change, Science, 316, 1735–1738, doi:10.1126/science.1136188, 2007. 10799

Liss, P. S. and Merlivat, L.: The Role of Air-Sea Exchange in Geochemical Cycling, chap. Air-sea gas exchange rates: Introduction and Synthesis, D. Reidel, Dordrecht, Netherlands, 113–127, 1986. 10802

Lohmann, K., Drange, H., and Bentsen, M.: Response of the North Atlantic subpolar gyre to persistent North Atlantic Oscillation like forcing, Clim. Dynam., 32, 273–285, doi:10.1007/s00382-008-0467-6, 2009. 10800

Maier-Reimer, E., Mikolajewicz, U., and Hasselmann, K.: Mean circulation of the Hamburg LSG OGCM and its sensitivity to the thermohaline surface forcing, J. Phys. Oceanogr., 23, 731–757, 1993. 10800

Maier-Reimer, E., Kriest, I., Segscheider, J., and Wetzel, P.: The HAMburg Ocean Carbon Cicle model HAMOCC5.1 – Technical description release 1.1, in: Berichte zur Erdsystemforschung, Tech. Rep. 14, Max Planck Institute for Meteorology, Hamburg, Germany, 2005. 10800, 10802

Meehl, G. A., Stocker, T. F., Collins, W. D., Friedlingstein, P., Gaye, A. T., Gregory, J. M., Kitoh, A., Knutti, R., Murphy, J. M., Noda, A., Raper, S. C. B., Watterson, I. G., Weaver, A. J., and Zhao, Z. C.: Climate Change 2007: The Physical Science Basis. Contribution of Working Group I to the Fourth Assessment Report of the Intergovernmental Panel on Climate

BGD
8, 10797–10821, 2011

Change, chap. Global Climate Projections, Cambridge University Press, Cambridge, United Kingdom and New York, NY, USA, 2007. 10799

Nightingale, P., Malin, G., Law, C., Watson, A., Liss, P., Liddicoat, M., Boutin, J., and Upstill-Goddard, R.: In situ evaluation of air-sea gas exchange parameterizations using novel conservative and volatile tracers, Global Biochem. Cy., 14, 373–387, 2000. 10802

Sabine, C. L., Feely, R. A., Gruber, N., Key, R. M., Lee, K., Bullister, J. L., Wanninkhof, R., Wong, C. S., Wallace, D. W. R., Tilbrook, B., Millero, F. J., Peng, T.-H., Kozyr, A., Ono, T., and Rios, A. F.: The oceanic sink for anthropogenic CO_2, Science, 305, 367–371, doi:10.1126/science.1097403, 2004. 10799

Schuster, U. and Watson, A. J.: A variable and decreasing sink for atrmospheric CO_2 in the North Atlantic, J. Geophys. Res., 112, C11006, doi:10.1029/2006JC003941, 2007. 10799

Six, K. D. and Maier-Reimer, E.: Effects of plankton dynamics on seasonal carbon fluxes in an ocean general circulation model, Global Biochem. Cy., 10, 559–583, doi:10.1029/96GB02561, 1996. 10800

Solomon, S., Quin, D., Manning, M., Chen, Z., Marquis, M., Averyt, K. B., Tignor, M., and Miller, H. L. (Eds.): Climate Change 2007. Contribution of Working Group I to the Fourth assessment Report of the Intergovernmental Panel on Climate Change, Cambridge University Press, Cambridge, United Kingdom and New York, NY, USA, 2007. 10798

Stow, C. A., Jolliff, J., McGillicuddy, D. J., Doney, S. C., Allen, J. I., Friedrichs, M. A. M., Rose, K. A., and Wallhead, P.: Skill assessment for coupled biological/physical models of marine systems, J. Marine Syst., 76, 4–15, doi:10.1016/j.jmarsys.2008.03.011, 2009. 10806, 10807

Sweeney, C., Gloor, E., Jacobson, A. R., Key, R. M., McKinley, G., Sarmiento, J. L., and Wanninkhof, R.: Constraining global air-sea gas exchange for CO_2 with recent bomb ^{14}C measurements, Global Biochem. Cy., 21, GB2015, doi:10.1029/2006GB002784, 2007. 10802

Takahashi, T., Sutherland, S. C., Wanninkhof, R., Sweeney, C., Feely, R. A., Chipman, D. W., Hales, B., Friederich, G., Chavez, F., Sabine, C., Watson, A. J., Bakker, D. C. E., Schuster, U., Metzl, N., Yoshikawa-Inoue, H., Ishii, M., Midorikawa, T., Nojiri, Y., Körtzinger, A., Steinhoff, T., Hoppema, M., Olafson, J., Arnarson, T. S., Tilbrook, B., Johannessen, T., Olsen, A., Bellerby, R., Wong, C. S., Delille, B., Bates, N. R., and de Baar, H. J. W.: Climatological mean and decadal change in surface ocean pCO_2, and net sea-air CO_2 flux over the global oceans, Deep-Sea Res. Pt. II, 56, 554–577, 2009. 10803, 10805, 10806, 10808, 10814, 10815, 10821

Tjiputra, J. F., Assmann, K., and Heinze, C.: Anthropogenic carbon dynamics in the changing

BGD
8, 10797–10821, 2011

ocean, Ocean Sci., 6, 605–614, doi:10.5194/os-6-605-2010, 2010. 10799
Trenberth, K. E., Jones, P. D., Ambenje, P., Bojariu, R., Easterling, D., Klein Tank, A., Parker, D., Rahimzadeh, F., Renwick, J. A., Rusticucci, M., Soden, B., and Zhai, P.: Climate Change 2007: The Physical Science Basis. Contribution of Working Group I to the Fourth Assessment Report of the Intergovernmental Panel on Climate Change, chap. Observations: Surface and Atmospheric Climate Change, Cambridge University Press, Cambridge, United Kingdom and New York, NY, USA, 2007. 10799
Wanninkhof, R.: Relation between wind speed and gas exchange over the ocean, J. Geophys. Res., 97, 7373–7383, 1992. 10802
Wanninkhof, R. and McGillis, W.: A cubic relationship between air-sea CO_2 exchange and wind speed, Geophys. Res. Lett., 26, 1889–1892, 1999. 10802
Wanninkhof, R., Asher, W. E., Ho, D., Sweeney, C., and McGillis, W. R.: Advances in Quantifying Air-Sea Gas Exchange and Environmental Forcing, Annual Review of Marine Science, 1, 213–244, doi:10.1146/annurev.marine.010908.163742, 2009. 10801, 10808
Watson, A. J., Schuster, U., Bakker, D. C. E., Bates, N. R., Corbière, A., González-Dávila, M., Friedrich, T., Hauck, J., Heinze, C., Johannessen, T., Körtzinger, A., Metzl, N., Olafsson, J., Olsen, A., Oschlies, A., Padin, X. A., Pfeil, B., Santana-Casiano, J. M., Steinhoff, T., Telszewski, M., Rios, A. F., Wallace, D. W. R., and Wanninkhof, R.: Tracking the variable North Atlantic sink for atmospheric CO_2, Science, 326, 1391–3, doi:10.1126/science.1177394, 2009. 10799
Weiss, R. F.: Carbon Dioxide in Water and Seawater: The Solubility of a Non-Ideal Gas, Mar. Chem., 2, 203–215, 1974. 10801
Woolf, D. K.: The Sea Surface and Global Change, chap. Bubbles and their role in gas exchange, Cambridge University Press, 173–205, 1997. 10808
Zickfeld, K., Fyfe, J. C., Saenko, O. A., Eby, M., and Weaver, A. J.: Response of the global carbon cycle to human-induced changes in Southern Hemisphere winds, Geophys. Res. Lett., 34, L12712, doi:10.1029/2006GL028797, 2007. 10799

BGD
8, 10797–10821, 2011

Table 1. Description of the model simulations performed in this work.

Experiment	Description
G01	Model standard run
G02	+44 % gas exchange rate between 40–60° N
G03	+44 % gas exchange rate polewards of 40° S
G04	+44 % gas exchange rate between 20° S–20° N

BGD
8, 10797–10821, 2011

Table 2. Summary of the global integrated carbon fluxes for the reference year 2000 and the best estimation from Takahashi et al. (2009).

Experiment	Upward flux [PgC]	Downward flux [PgC]	Net flux [PgC]
Standard run (G01)	92.3785	–94.8434	–2.4649
Increasing gas exchange rate between 40–60° N (G02)	96.7672	–99.2654	–2.4881
Increasing gas exchange rate polewards of 40° S (G03)	107.0329	–109.4042	–2.3713
Increasing gas exchange rate between 20° S–20° N (G04)	102.3120	–104.7883	–2.4763
Takahashi et al. (2009)	–	–	-1.6 ± 0.9

BGD
8, 10797–10821, 2011

Table 3. Statistical analysis for the reference year 2000 compared to the best estimation from Takahashi et al. (2009) in the experimental areas for both zonally averaged CO_2 fluxes and the pCO_2.

Parameter	Experiment	correlation coefficient	root mean squared error	average absolute error	model efficiency
CO_2 flux	Standard run	0.967	41.90	6.26	−0.12
	G02	0.969	53.44	6.80	−0.83
	Standard run	−0.364	176.15	12.28	−1.31
	G03 (40–60° S)	−0.138	164.08	11.94	−1.01
	Standard run	0.892	40.42	5.97	0.61
	G04	0.899	35.74	5.68	0.70
pCO_2	Standard run	0.785	5.61	2.16	−1.12
	G02	0.750	9.05	2.97	−4.51
	Standard run	−0.793	11.96	3.11	−1.37
	G03 (40–60° S)	−0.695	13.23	3.14	−1.90
	Standard run	0.934	14.59	3.61	−0.07
	G04	0.935	12.52	3.37	0.21

BGD
8, 10797–10821, 2011

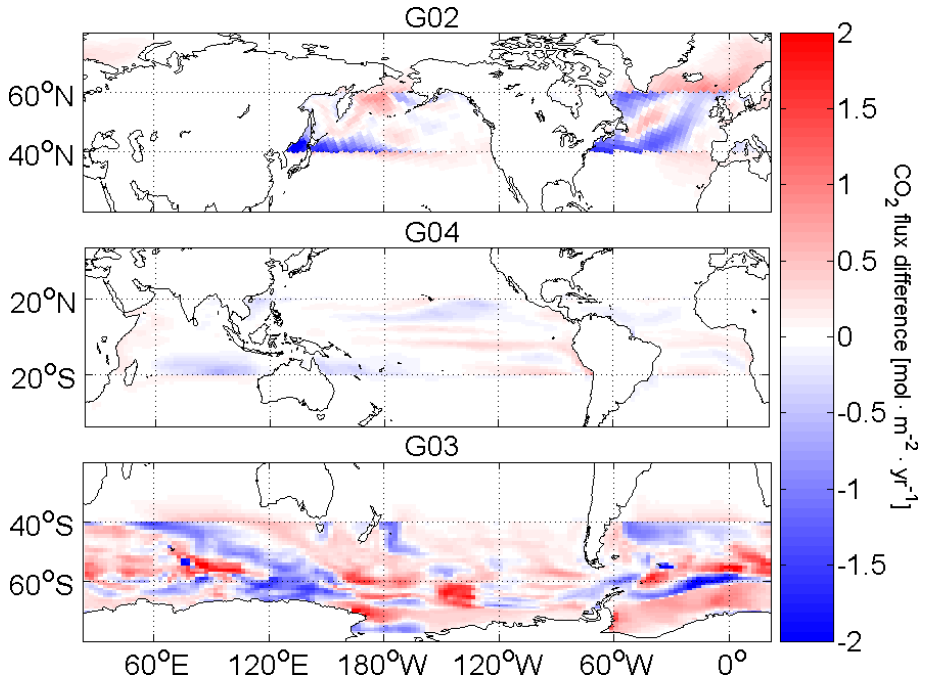

Fig. 1. Annual surface flux difference between the model standard run and the G02 scenario (top), the G04 scenario (middle) and the G03 scenario (bottom) in molC m^{-2} yr^{-1} for the reference year 2000. Negative values describe increasing uptake fluxes and positive values describe decreasing uptake compared to the standard run.

BGD
8, 10797–10821, 2011

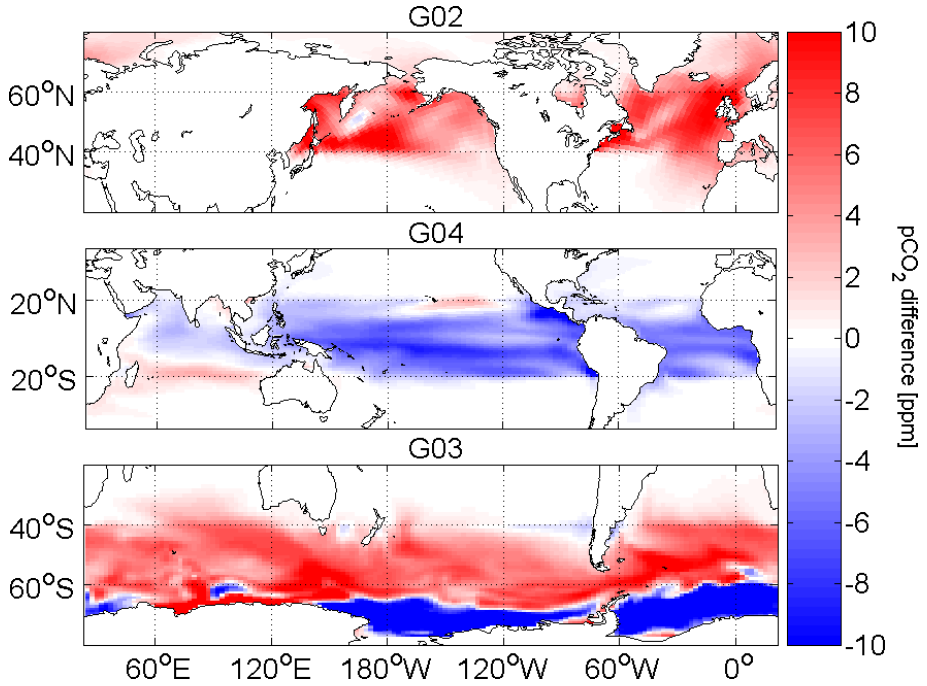

Fig. 2. Annual pCO_2 difference between the model standard run and the G02 scenario (top), the G04 scenario (middle) and the G03 scenario (bottom) in ppm for the reference year 2000. Negative values describe lower pCO_2 concentrations, whereas positive values show increasing partial pressures compared to the standard run.

BGD
8, 10797–10821, 2011

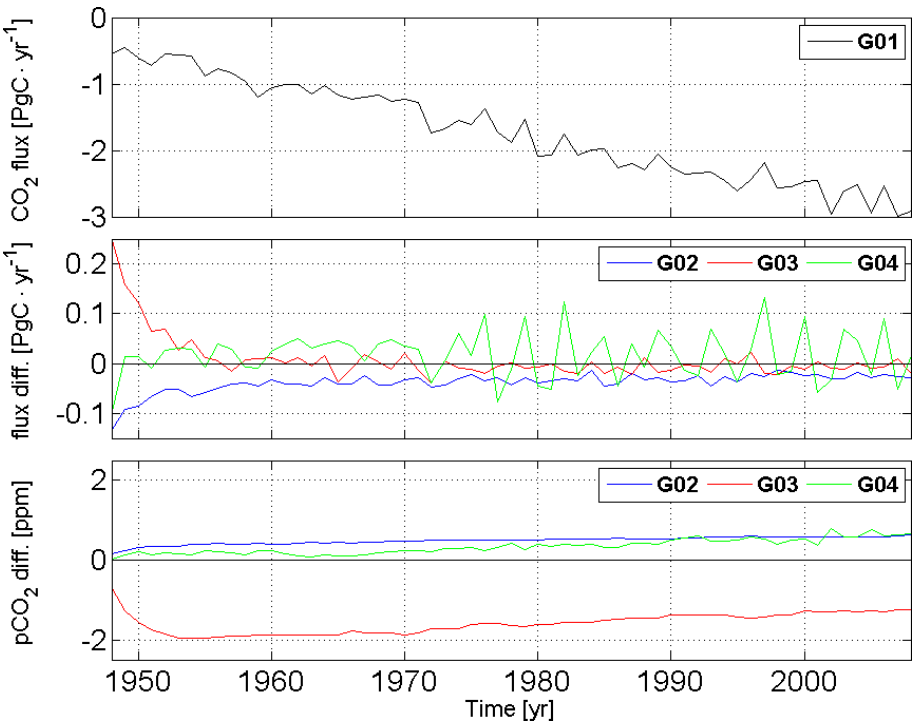

Fig. 3. Annual global integrated sea-air carbon flux simulated by G01 in PgC yr^{-1} (top). Difference in the global integrated carbon flux between the sensitivity scenarios and the model standard run in PgC yr^{-1} (middle). Difference in the global mean surface pCO_2 between the sensitivity scenarios and the model standard run in ppm (bottom).

BGD
8, 10797–10821, 2011

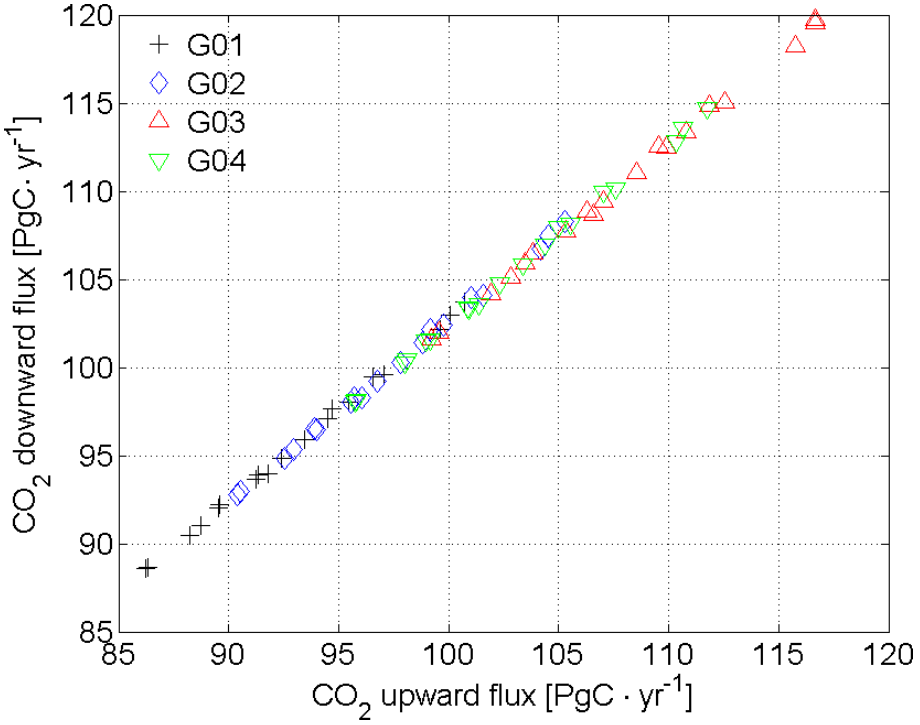

Fig. 4. Global integrated annual upward versus downward flux plot from year 1990 onwards for all model runs.

BGD
8, 10797–10821, 2011

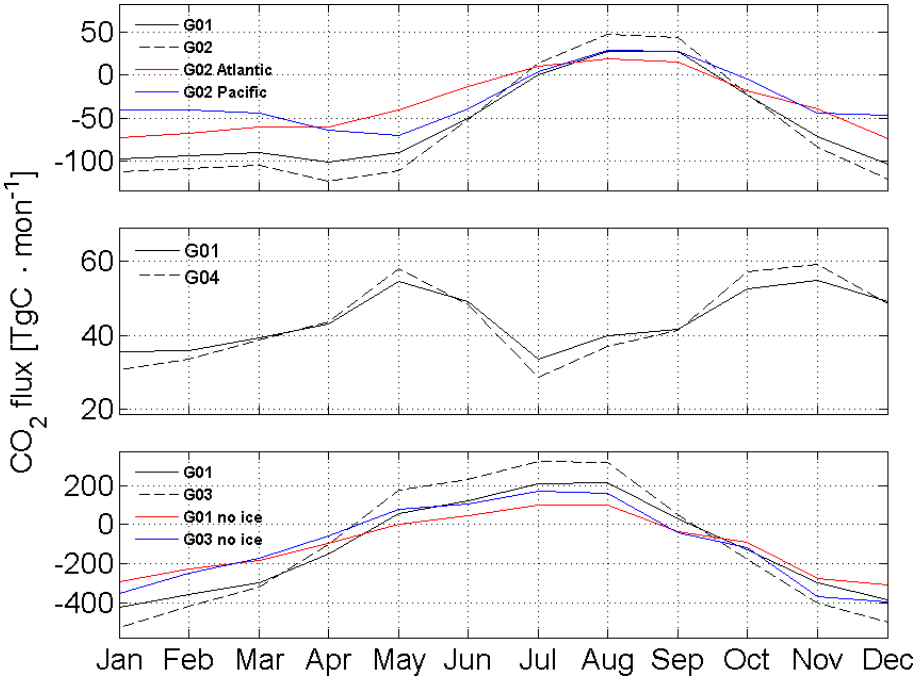

Fig. 5. Monthly mean (for the year 2000) CO_2 fluxes for the model standard run between 40–60° N (top), 20° S–20° N (middle) and south of 40° S (bottom) in TgC mon^{-1}. Negative fluxes describe CO_2 uptake by the ocean.

BGD
8, 10797–10821, 2011

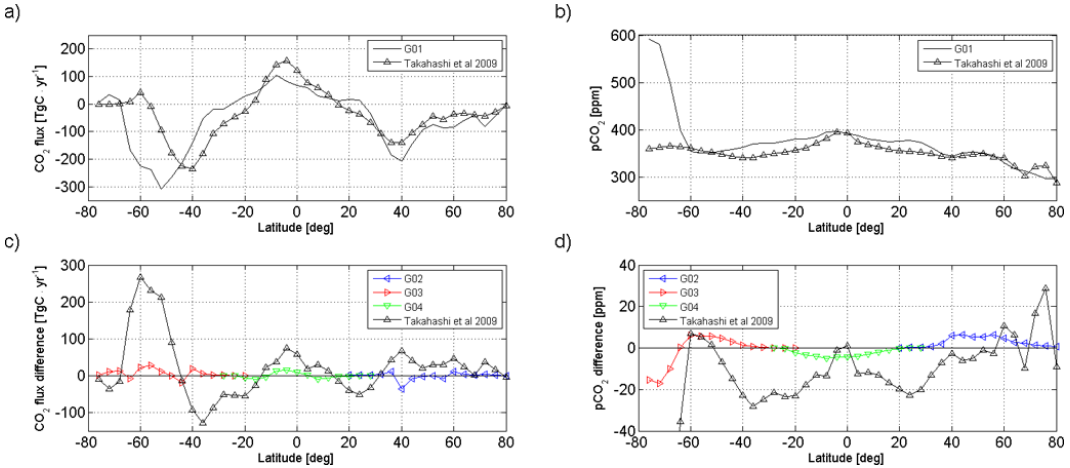

Fig. 6. Comparison of the zonally averaged **(a)** CO_2 flux and **(b)** pCO_2 between the standard run (G01) from year 2000 and the climatology of Takahashi et al. (2009). Latitudinal difference of the **(c)** CO_2 fluxes and **(d)** pCO_2 between the different sensitivity experiments with the standard run (G01). Difference between the observation and G01 is also included. Values shown here are mean computed over 4 degree zonal band, in units of TgC yr^{-1} for the CO_2 flux and ppm for the pCO_2.

BGD
8, 10797–10821, 2011

A model study on the sensitivity of surface ocean CO_2 pressure

P. Landschützer et al.